42 Sokol, C. L., Chu, N. Q., Yu, S., Nish, S. A., Laufer, T. M. and Medzhitov, R. 2009. Basophils function as antigen-presenting cells for an allergen-induced T helper type 2 response. *Nat. Immunol.* 10:713.
43 Yoshimoto, T., Min, B., Sugimoto, T. *et al.* 2003. Nonredundant roles for CD1d-restricted natural killer T cells and conventional CD4+ T cells in the induction of immunoglobulin E antibodies in response to interleukin 18 treatment of mice. *J. Exp. Med.* 197:997.
44 Ishikawa, Y., Yoshimoto, T. and Nakanishi, K. 2006. Contribution of IL-18-induced innate T cell activation to airway inflammation with mucus hypersecretion and airway hyperresponsiveness. *Int. Immunol.* 18:847.

Insect Molecular Biology

Insect Molecular Biology (2012)

doi: 10.1111/j.1365-2583.2011.01128.x

Induction of antisporozoite antibodies by biting of transgenic *Anopheles stephensi* delivering malarial antigen via blood feeding

D. S. Yamamoto*, M. Sumitani*, H. Nagumo*, S. Yoshida† and H. Matsuoka*

**Division of Medical Zoology, Department of Infection and Immunity, Jichi Medical University, Yakushiji, Shimotsuke, Tochigi, Japan; and †Laboratory of Vaccinology and Applied Immunology, Kanazawa University School of Pharmacy, Kakuma-machi, Kanazawa, Ishikawa, Japan*

Abstract

We produced a transgenic mosquito expressing a rodent malaria vaccine candidate antigen in the salivary gland. Three tandemly repeated amino acid units from the repeat region of circumsporozoite protein of *Plasmodium berghei* (PbCS3R) fused to red fluorescent protein (monomeric DsRed) was chosen as a vaccine candidate antigen. Immunoblot and fluorescence microscopic analyses showed the transgene expression in the female salivary gland. The transgene product was released from the proboscis as a component of saliva. The monomeric DsRed-fusion expression system could be suitable for transgene secretion in the saliva of female mosquitoes. Mice repeatedly bitten by transgenic mosquitoes raised antibodies against *P. berghei* sporozoites, and the sera had protective ability against sporozoite invasion of human hepatoma HepG2 cells. These results suggest that transgene products are immunogenically active in saliva, and induce the antibodies to malaria parasite. These findings indicate that this technology has the potential for production of a 'flying vaccinator' for rodent malaria parasites.

Keywords: mosquito, salivary gland, malaria, transgenesis, circumsporozoite protein.

Correspondence: Daisuke S. Yamamoto, Department of Infection and Immunity, Division of Medical Zoology, Jichi Medical University, Yakushiji, Shimotsuke 329-0498, Japan. Tel.: + 81 285 58 7339; fax: + 81 285 44 6489; e-mail: daisukey@jichi.ac.jp

Introduction

Transgenesis is a general tool for functional analysis of genes, and this technique has been successfully applied in more than 20 insect species (Handler & O'Brochta, 2009). Transgenic techniques have been developed in mosquitoes, which transmit diseases such as malaria, dengue and yellow fever (Chen *et al.*, 2008). Genomic sequence has been studied in some mosquitoes (Holt *et al.*, 2002; Nene *et al.*, 2007) and the use of comprehensive gene expression analysis has also been studied in some mosquito tissues (Bonnet *et al.*, 2001; Francischetti *et al.*, 2002; Sanders *et al.*, 2003; Valenzuela *et al.*, 2003; Arca *et al.*, 2005; Ribeiro *et al.*, 2007). In addition, gene knockdown systems (RNA interference, RNAi) have been established in adult mosquitoes (Blandin *et al.*, 2002), and it has been shown that transgenic RNAi, which involves a combination of transgenesis and RNAi, is effective for analysis of the function of genes in mosquitoes (Brown *et al.*, 2003). Thus, mosquito transgenesis is expected to be a powerful tool for the analysis of vector–parasite interactions. Moreover, it is possible that transgenic mosquitoes can be used as a strategy to control infectious disease (Terenius *et al.*, 2008), by the application of some mosquito lines expressing parasite-refractory molecules to malaria parasite or dengue virus (Ito *et al.*, 2002; Yoshida *et al.*, 2007; Rodrigues *et al.*, 2008; Mathur *et al.*, 2010; Isaacs *et al.*, 2011).

Additionally, insect transgenesis has been used for the cost-effective mass production of useful recombinant proteins. In insect cells, recombinant proteins have been synthesized with post-translational modifications such as disulphide bond formation, multisubunit complex formation and glycosylation compared with the expression systems of recombinant proteins using microorganisms (Kost *et al.*, 2005). Recently, insect cell (eg Sf-9) and baculovirus (*Autographa california* nucleopolyhedrosis virus) expression systems have been used to produce valuable proteins for many applications including vaccine candidate antigens (Kost *et al.*, 2005; Yoshida *et al.*, 2009, 2010a, b). In the transgenic silkworm *Bombyx mori*, a silk

gland expression system has been established as a tool for mass production of therapeutic and industrially relevant recombinant proteins (Tomita, 2011). In mosquitoes, the concept of using transgenic mosquitoes to deliver therapeutic molecules has been proposed, which is known as the 'flying syringe' or 'flying vaccinator' in the case of delivering vaccine molecules (Crampton *et al.*, 1999). In mosquito saliva, there are a number of proteins such as anticlotting molecules, antiplatelet aggregation molecules and vasodilators (Ribeiro *et al.*, 2010), and it is known that these proteins are injected into the host skin by mosquitoes via blood feeding and antibodies against the saliva proteins are then induced (Waitayakul *et al.*, 2006). On the basis of these findings, it is possible that vaccine candidate molecules could be produced under near-native conditions in the transgenic mosquito salivary glands compared with those in microorganism expression systems and that transgenic mosquitoes expressing vaccine candidate antigens in saliva could immunize the host via blood-feeding. We have established a system of female salivary gland-specific gene expression in transgenic *Anopheles stephensi* mosquitoes using the promoter region of *anopheline antiplatelet protein* (*aapp*) gene, which encodes an inhibitor of collagen-induced antiplatelet aggregation (Yoshida & Watanabe, 2006; Yoshida *et al.*, 2008; Matsuoka *et al.*, 2010). Recently, we established the 'flying vaccinator' technology and generated transgenic mosquitoes that deliver a *Leishmania* vaccine candidate antigen in *A. stephensi* (Yamamoto *et al.*, 2010).

In this study, we applied this technology for delivery of a malaria vaccine candidate antigen in a mouse model system. We focused on the circumsporozoite protein (CSP) as a malaria vaccine candidate antigen. The CSP is expressed on the surface of the sporozoite, and is known as one of the leading human malaria vaccine candidates (Alonso *et al.*, 2004; Bejon *et al.*, 2008). It has been shown that antibodies to the repeat region of the CSP of a human malaria parasite, *Plasmodium falciparum*, have the ability to inhibit sporozoite invasion into hepatocytes (Hollingdale *et al.*, 1984). In some studies using rodent malaria parasites, *Plasmodium berghei* and *Plasmodium yoelii*, mice immunized with conjugates of synthetic peptides of the CSP repeat region and carrier protein or with multiple antigen peptides (MAPs) representing *P. berghei* CSP repeats had full protection against challenge with sporozoites (Egan *et al.*, 1987; Zavala *et al.*, 1987; Tam *et al.*, 1990; Wang *et al.*, 1995). In a previous study, we produced transgenic mosquitoes expressing the near full-length *P. berghei* CSP in female salivary glands; however, this CSP was not secreted into the saliva (Matsuoka *et al.*, 2010). We raised the possibility that red fluorescent protein (monomeric DsRed)-fusion expression system stabilizes and/or chaperones transgene products in the female salivary gland (Yamamoto *et al.*, 2010). Therefore, in this study, the gene encoding three tandemly repeated amino acid units from the repeat region of the *P. berghei* CSP (PbCS3R) fused to monomeric DsRed was inserted into the *A. stephensi* genome. Expression of the transgene protein was analysed in the salivary gland of the transgenic mosquitoes, and sera from mice bitten repeatedly by these mosquitoes were analysed. From the obtained results, we discuss the potential of this transgenic mosquito as a 'flying vaccinator' against malaria.

Results and discussion

Generation of transgenic line

A *Minos*-based transfer vector plasmid comprising a gene cassette consisting of the three tandemly repeated amino acid units of PbCS3R fused to monomeric DsRed (*DsRed-PbCS3R*) under the control of the *aapp* promoter (Fig. 1) was injected together with a *Minos* helper plasmid into *A. stephensi* embryos. Seventy-six embryos of the 251 injected (30%) hatched normally and of these, 47 adults emerged. Four independent transgenic lines were established from these adults. A single integration event was confirmed by Southern blot analysis (Fig. S1). The four transgenic lines have been stably maintained by blood-meals on mice for over 10 generations.

Transgene products in the salivary glands

Immunoblot analyses of all four transgenic lines with anti-*P. berghei* CSP (PbCSP) antibody, 3D11 mouse monoclonal antibody (mAb), were used to verify the presence of expressed DsRed-PbCS3R protein (M_r = 35 kDa) in the salivary glands (Fig. 2A). The expression levels of DsRed-PbCS3R protein in the salivary glands were the highest in line 3 amongst the four lines following calibration with anti-AAPP-antibody recognition of native AAPP (M_r = 37 kDa). Therefore, line 3 was used in all further analyses. The amount of DsRed-PbCS3R protein expressed was estimated as approximately 10 ng per pair of salivary glands, as quantified by comparison with monomeric DsRed protein (M_r = 30 kDa) (Fig. 2B). This expression level was equivalent to as much as 2% of the total salivary gland protein (Yoshida & Watanabe, 2006).

Red fluorescence was observed in the distal-lateral lobe of female salivary glands of DsRed-PbCS3R mosquitoes (Fig. 3A, B). To counterstain for secretory cells, the distal-lateral lobes were stained with SYTO-13, which stains DNA and RNA in live cells. Red fluorescence was observed in secretory cavities and ducts of the distal-lateral lobes as well as secretory cells under confocal fluorescent microscopy (Fig. 3C–E). These results indicate that the transgene product, DsRed-PbCS3R protein, was located in salivary acini. Moreover, to determine

A

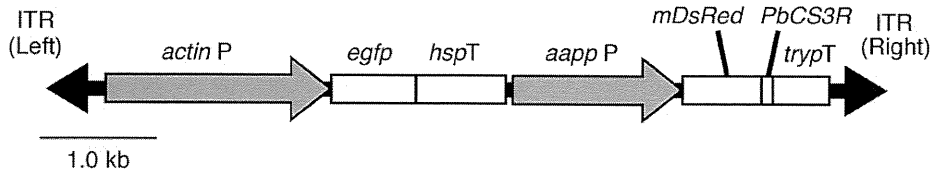

B

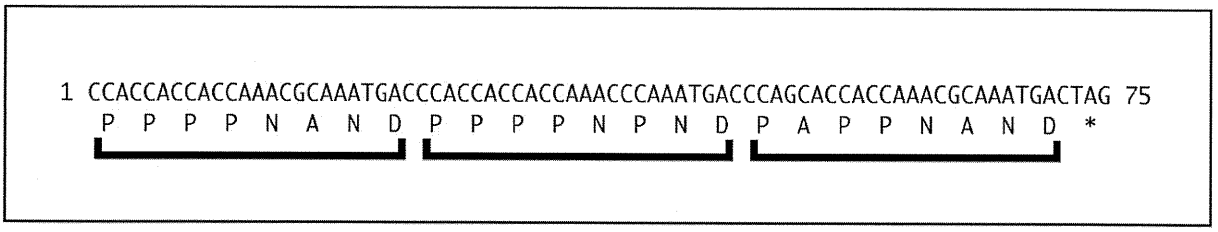

Figure 1. Schematic representation of genomic structure of the DsRed-PbCS3R mosquito. (A) Schematic representation of genomic structure of the DsRed-PbCS3R mosquito. ITR, *Minos* inverted terminal repeat; *actin*P, *Drosophila melanogaster actin5c* promoter; *egfp*, enhanced green fluorescent protein-coding sequence; *hsp*T, *D. melanogaster* terminator sequence; *aapp*P, *Anopheles stephensi anopheline antiplatelet protein* regulatory elements; *mDsRed*, monomeric DsRed-coding sequence; PbCS3R, repeat region of *Plasmodium berghei* circumsporozoite protein-coding sequence; trypT, *Anopheles gambiae trypsin* terminator sequence. (B) Sequence of *PbCS3R* gene. Amino acid sequence is shown below. Asterisk: stop codon. Clamps: repeat amino acid units of *P. berghei* circumsporozoite protein.

whether DsRed-PbCS3R protein was released from the proboscis with saliva, salivation of the transgenic mosquitoes and wild-type mosquitoes was monitored under fluorescent microscopy, and the release of red fluorescence from the proboscis in transgenic mosquitoes was identified (Fig. 3F). The localization pattern and salivation of transgene product were consistent with the results for *Leishmania* 'flying vaccinator' mosquitoes, which expressed the transgene product, DsRed-SP15 protein, upon use of the same expression cassette including the *aapp* promoter and monomeric DsRed tag as in other transgenic mosquitoes (Yamamoto *et al.*, 2010). These results suggest that DsRed-PbCS3R protein is released as a component of saliva from the proboscis during salivation. In a previous study, the *P. berghei* CSP without a signal peptide region and C-terminal glycosylphosphatidylinositol (GPI)-anchor domain, which was not fused to monomeric DsRed protein (M_r = 38 kDa), was expressed in the salivary gland cells, but the CSP was not secreted into the saliva in transgenic *A. stephensi* (Matsuoka *et al.*, 2010). Together, these findings indicate that the CSP including the entire repeat region may not be suitable for protein folding in the mosquito salivary gland and/or secretion into the saliva. In addition, the monomeric DsRed-fusion expression system may chaperone transgene products in the female salivary gland, as described by Yamamoto *et al.* (2010).

Antibody responses to PbCSP in sera of mice exposed to transgenic mosquitoes

We tested whether these mosquitoes could deliver DsRed-PbCS3R protein to the host during blood-feeding. The sera from four mice repeatedly bitten by about 1500 DsRed-PbCS3R or wild-type (WT) mosquitoes were analysed by immunoblot analysis. It is known that anti-PbCSP antibody, 3D11 mAb specific for PbCSP repeats, recognized three polypeptides (44, 52 and 54 kDa) of CSP in sporozoites from midguts and salivary glands (Yoshida *et al.*, 1981). The 44 and 54 kDa forms are major molecules, and the 52 and 54 kDa forms are considered to be the intercellular precursor of CSP (Yoshida *et al.*, 1981; Thathy *et al.*, 2002). Similarly, the sera from two of the four mice (mice nos 2 and 3) specifically recognized the two major forms and the one minor form of CSP in the *P. berghei*-infected midgut (Fig. 4A). In contrast, none of the sera from mice repeatedly bitten by WT mosquitoes recognized CSP. Anti-PbCSP antibody titres of the sera from mice repeatedly bitten by DsRed-PbCS3R mosquitoes were determined by enzyme-linked immunosorbent assay (ELISA) using synthetic peptides of the repeat region of PbCSP (syPbCSP; Fig. 4B). The sera from two of the four mice (mice nos 2 and 3) repeatedly bitten by transgenic (TG) mosquitoes reacted with syPbCSP. One of these two mice raised a high level of anti-syPbCSP

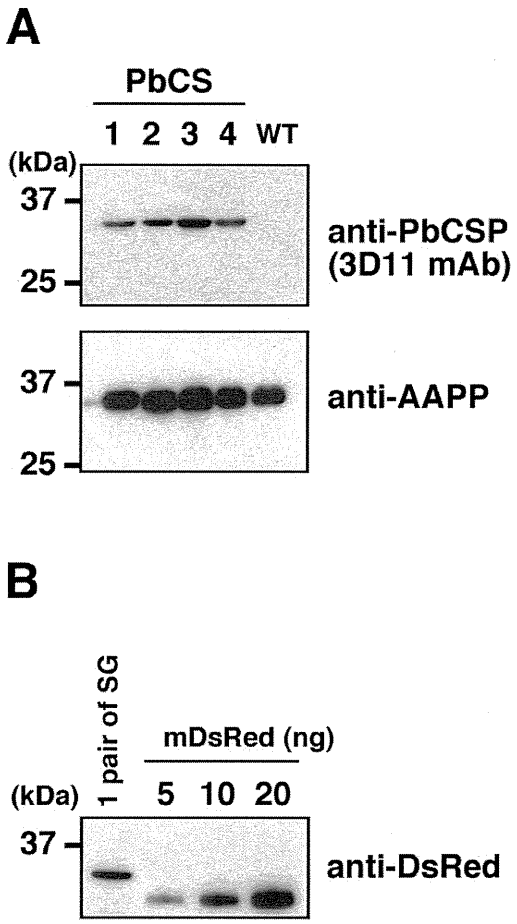

Figure 2. Immunoblotting of DsRed-PbCS3R protein in the salivary glands (SGs). (A) The five pairs of female SGs of four DsRed-PbCS3R transgenic lines (PbCS, 1–4) and wild-type (WT) mosquitoes were analysed using anti-*Plasmodium berghei* circumsporozoite protein [3D11 mouse monoclonal antibody (3D11 mAb)] and anti-anopheline antiplatelet protein (anti-AAPP) antibodies. (B) Estimation of the amount of DsRed-PbCS3R in the salivary glands. The one pair of female SGs of DsRed-PbCS3R transgenic line 3 and recombinant monomeric DsRed proteins (mDsRed) were analysed using anti-DsRed antibody. The amount of mDsRed (5, 10, 20 ng) is indicated at the top of each lane.

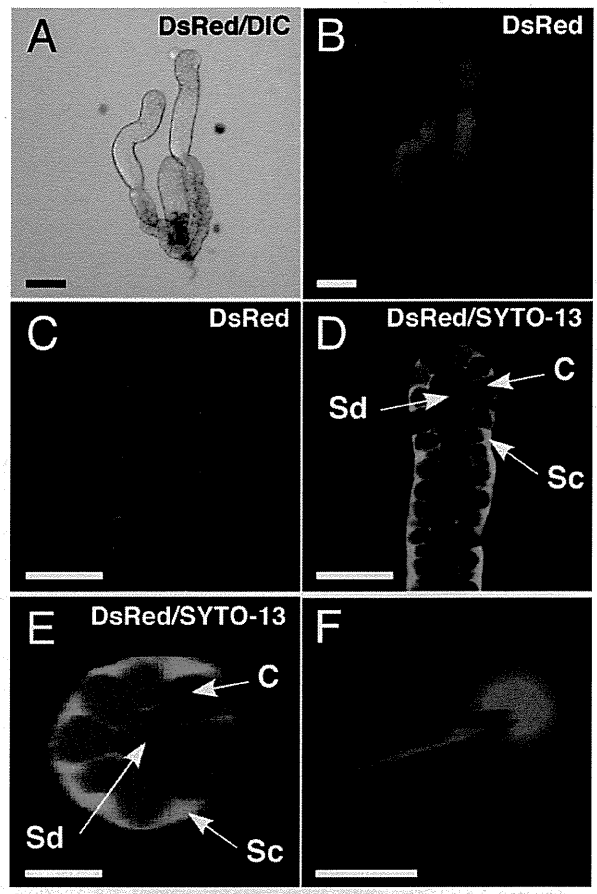

Figure 3. Localization of transgene products in salivary gland. 3D confocal imaging of the dissected salivary glands from female DsRed-PbCS3R mosquitoes (A–E). (A) Overlay image of the DsRed fluorescence and differential interference contrast (DIC) of the salivary gland of DsRed-PbCS3R mosquito. Red fluorescence was observed in the distal-lateral lobes of the female salivary glands of transgenic mosquito. (B) DsRed fluorescence image of the salivary gland of DsRed-PbCS3R mosquito. A longitudinal section (C and D) and cross-section (E) of the distal-lateral lobe of DsRed-PbCS3R mosquito stained with SYTO-13 green-fluorescent dye to counterstain for secretory cells. DsRed fluorescence image (C) and overlay image of the DsRed and SYTO-13 fluorescence (D and E). C, salivary cavity; Sc, secretory cell; Sd, salivary duct. (F) Saliva with red fluorescence during salivation from the proboscis of DsRed-PbCS3R mosquitoes was released. Scale bars = 100 μm (A, B), 50 μm (C, D), 25 μm (E) and 200 μm (F).

Figure 4. Anti-*Plasmodium berghei* circumsporozoite protein (anti-PbCSP) antibody responses in individual mice bitten repeatedly by DsRed-PbCS3R mosquitoes. (A) Immunoblotting of individual sera. A total of about 1500 DsRed-PbCS3R (transgenic, TG) or wild-type (WT) mosquitoes were allowed to feed on each mouse over four months. Numbers indicate individual mice bitten by TG (nos 1–4) or WT (nos 5–8) mosquitoes. Sera diluted to 1:500 were used to react with midgut extract from mosquitoes infected with *P. berghei*. 3D11 monoclonal antibody was used as a positive control (left lane). Naïve mouse serum diluted to 1:500 was used as a negative control (right lane). The result of immunoblotting using anti-*P. berghei* heat shock protein 70 (HSP70) antibody is shown below. (B) Anti-synthetic peptides of the repeat region of PbCSP (anti-syPbCSP) antibody titres of sera obtained from mice (nos 1–8) specific for syPbCSP. Twofold serial dilutions of sera started at 1:100. Anti-syPbCSP antibody titre of sera from mouse no.5 was not at a detectable level (<100). Bars indicate the means of antibody titres. (C) Antisalivary gland protein antibody titres of sera obtained from mice (nos 1–8) specific for salivary gland extract. Twofold serial dilutions of sera started at 1:1000. Bars indicate the means of antibody titres. (D) Immunofluorescence assay of *P. berghei* sporozoites dissected from salivary glands using sera from mice repeatedly bitten by TG mosquitoes (mouse no. 2) and WT mosquitoes (mouse no. 6). 3D11 monoclonal antibody was used as a positive control. DNA was stained with DAPI. BF, bright field. Scale bars = 10 μm.

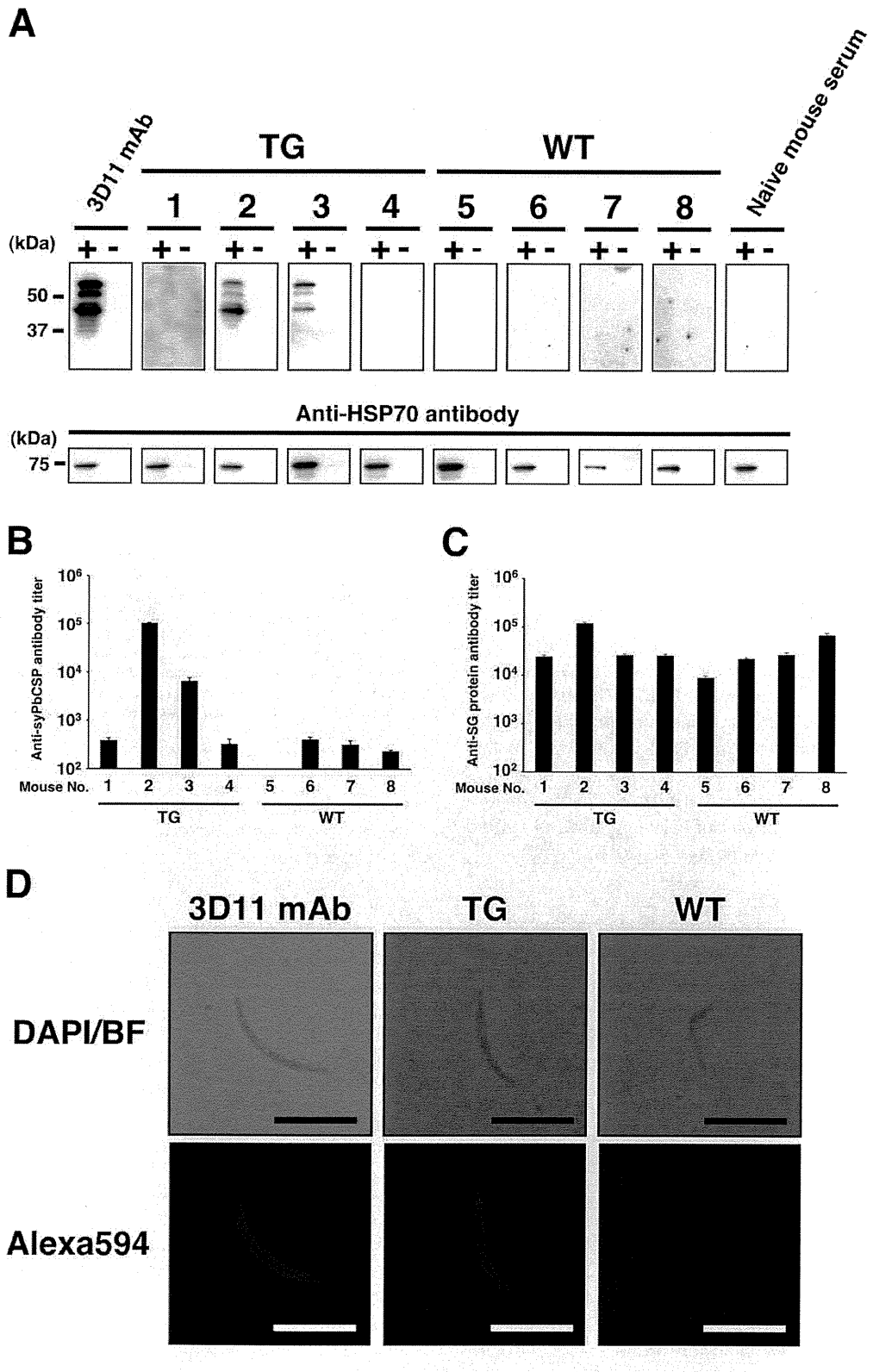

antibodies. In contrast, all of the sera from the mice repeatedly bitten by WT mosquitoes reacted with a salivary gland extract (Fig. 4C). The results of ELISA analyses were consistent with the results of the immunoblot analyses. These results suggest that immunogenically active DsRed-PbCS3R was injected as a component of saliva during blood-feeding and induced the repeat region of PbCSP-specific antibodies. The results of fluorescent immunoassay support this (Fig. 4D). The serum from mouse no. 2 recognized the sporozoites similarly to 3D11 mAb.

In this study, two of the four mice repeatedly bitten by DsRed-PbCS3R mosquitoes raised antibody against the syPbCSP. In a previous study, however, we generated 'flying vaccinator' mosquitoes delivering *Leishmania* vaccine candidate antigen, SP15, which was derived from a saliva protein of the sandfly *Phlebotomus papatasi* (Yamamoto *et al.*, 2010). In SP15 transgenic mosquitoes, almost full-length SP15 protein fused to monomeric DsRed protein (DsRed-SP15) was expressed in the female salivary glands and delivered into mice via blood-feeding. The transgene products were similar monomeric DsRed fusion proteins in the DsRed-PbCS3R mosquitoes and DsRed-SP15 mosquitoes. Nevertheless, all of the four mice raised antibody against the recombinant SP15 proteins upon being repeatedly bitten by DsRed-SP15 mosquitoes (Yamamoto *et al.*, 2010). The difference in antibody response with blood-feeding between these two transgenic mosquito lines may have resulted from antigenicity between PbCS3R and SP15, or the amount of antigen fused to monomeric DsRed in saliva of transgenic mosquitoes (20 ng per pair of salivary glands of DsRed-SP15 mosquitoes; Yamamoto *et al.*, 2010).

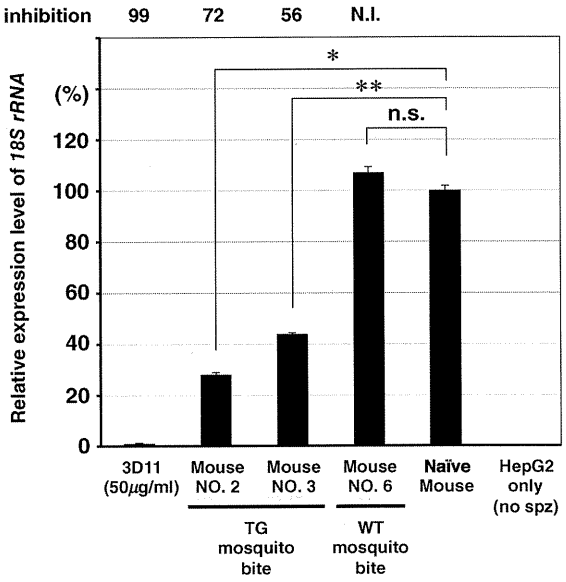

Figure 5. The relative expression level of *Plasmodium berghei 18S rRNA* associated with sera from mice repeatedly bitten by transgenic (TG) and wild-type (WT) mosquitoes using the sporozoite-neutralization assay. The sporozoite-neutralization assay was performed using sera from mice repeatedly bitten by DsRed-PbCS3R mosquitoes (no. 2, 3) or WT mosquitoes (no. 6). Fifty μg/μl of 3D11 mouse monoclonal antibody and naïve mouse sera were used as a positive control and a negative control, respectively. The relative level of *P. berghei* sporozoite 18S rRNA with naïve mouse serum was defined as 100%. Quantitative real-time PCR was performed three times using the templates. The p-value between the two groups was calculated by Welch's two sample t-test with Bonferroni correction. *, $P < 0.001$; **, $P < 0.01$; n.s., not significant. Percentage inhibition values have been indicated at the top of each bar. Percentage inhibition values were obtained using the following formula: 100-[relative level of *P. berghei* sporozoite *18S rRNA* (%)]. N.I., no inhibition; spz, sporozoite.

Protection against P. berghei *sporozoite infection in human hepatoma HepG2 cells*

To evaluate the protective ability of the sera from mice repeatedly bitten by DsRed-PbCS3R mosquitoes, the sera from mice (mice nos 2 and 3) that reacted with sporozoites were examined using sporozoite-neutralizing assay. The sera blocked the sporozoite invasion of HepG2 cells (Fig. 5). The *P. berghei* rRNA levels in the sera from mouse no. 2 and mouse no. 3 that had been repeatedly bitten by DsRed-PbCS3R mosquitoes were markedly reduced to 28 and 44.0% of *P. berghei* rRNA level in the serum from naïve mouse, respectively. This result indicates that these sera inhibited the sporozoite infection in HepG2 cells (72 and 56%, respectively). However, these *P. berghei* rRNA levels were higher than the levels (1%) with 50 μg/ml of mAb 3D11 specific for PbCSP repeats (99% inhibition of the sporozoite infection in HepG2 cells). In contrast, the *P. berghei* rRNA levels in the serum from a mouse (mouse no. 6) that had been repeatedly bitten by WT mosquitoes were not statistically different from the levels in naïve mouse serum. Similar results were obtained with another neutralization assay using the sera from mouse no. 2 and mouse no. 6 (Fig. S2). These results suggest that antibodies induced by DsRed-PbCS3R mosquito bite have protective ability against sporozoite invasion of hepatocytes, and DsRed-PbCS3R transgenic mosquitoes have the possibility to act as a 'flying vaccinator' against malaria sporozoites.

In the present study, because only two of four mice repeatedly bitten by DsRed-PbCS3R transgenic mosquitoes induced antibodies to the parasite, and one of the two mice induced a low serum titre of antibodies, the immunizing vaccine antigens for mosquitoes should be improved to induce the antibody efficiently. We are now proceeding to improve the vaccine antigens expressed in the transgenic mosquitoes and evaluate vaccine efficacy *in vivo* by *P. berghei* challenge with mosquito bites. In previous studies, mice immunized with conjugates of a synthetic

peptide representing a repeat region of *P. berghei* CSP and tetanus toxoid or keyhole limpet haemocyanin induced high serum titres of antibodies to the sporozoite; thus, most of these mice were protected from malaria infection when challenged intravenously with sporozoites (Egan *et al.*, 1987; Zavala *et al.*, 1987). The MAPs representing CSP repeats (B-cell epitopes) and T-cell epitopes at the C-terminal region of CSP in *P. berghei* induced high titres of antibodies to sporozoites and protective immunity against intravenous challenge of sporozoites, whereas antibodies to sporozoites were not induced by immunization of MAPs containing CSP repeats only (Tam *et al.*, 1990). Furthermore, RTS, S antigen, the most clinically advanced malaria vaccine candidate against *P. falciparum*, is based on part of the CSP amino acid sequence of *P. falciparum*, which bears NANP amino acid repeat B-cell epitope and T-cell epitope regions (Cohen *et al.*, 2010). Therefore, fusion proteins of peptide representing CSP di-epitopes (part of CSP repeats and T-cell epitopes) and monomeric DsRed may be suitable as vaccine antigens secreted in the saliva of 'flying vaccinator' mosquitoes. Furthermore, it has recently been found that the conformation and processing of the N-terminal region and C-terminal region of CSP are important for sporozoite adhesion to and invasion of hepatocytes, and region I at the N terminus of the repeat region plays a critical role in this process (Coppi *et al.*, 2011). Part of the N-terminal region or region I may also become vaccine antigens expressed in 'flying vaccinator' mosquitoes.

However, it remains unclear how many bites and how long a postexposure interval is needed to induce protective immunity in humans. In the case of mice, anti-PbCSP repeats antibody responses were induced following about 1500 bites over four months. In the Solomon Islands, a malaria hyperendemic area, the inhabitants are naturally bitten by over 100 anopheline mosquitoes per night (Hii *et al.*, 1993; Harada *et al.*, 1998). From these studies, it may be possible that continuous exposure to 'flying vaccinator' bites may naturally boost malaria immune responses. Further studies are needed to confirm the duration of antibody titre and the boosting effect by 'flying vaccinator' mosquitoes.

In summary, we have demonstrated that the antibodies to a rodent malaria parasite can be raised in mice after being bitten by transgenic mosquitoes. These findings constitute that this technology has the potential for production of a 'flying vaccinator' against malaria sporozoites. However, the 'flying vaccinator' mosquitoes should be refractory to malaria parasites. Thus, the gene construct expressing the vaccine antigens in saliva should be integrated together with a gene construct refractory to malaria parasites in mosquitoes. Alternatively, the technology of a 'flying vaccinator' could be applied to species of mosquitoes that do not transmit the malaria parasite. Moreover, public acceptance is essential prior to the use of transgenic mosquitoes. The dosage of vaccine antigens and involvement of only subjects who have provided informed consent cannot be controlled by vaccination with mosquitoes in the field. Therefore, solutions to these problems should be addressed before a 'flying vaccinator' is used. In the meantime, this idea may have potential for livestock disease control in isolated locations.

Experimental procedures

Animals

The *A. stephensi* mosquito strain SDA500 was maintained at 26 °C and 50–70% relative humidity under 13 h-light/11 h-dark conditions. Larvae were fed on tropical fish food (Kyorin, Himeji, Japan). Adults were fed on filter paper soaked with a 5% fructose and 0.05% *p*-aminobenzoic acid (Nacalai, Kyoto, Japan). Female ICR strain mice were obtained from Japan SLC (Hamamatsu, Shizuoka, Japan) and used at 8 weeks of age. *P. berghei* strain, ANKA, was maintained by cyclical passage through ICR mice and *A. stephensi* mosquitoes.

Minos *vector construction and germline transformation*

PCR reactions were performed with *Pfu* DNA polymerase (Stratagene GmbH, Heidelberg, Germany). A 762-bp DNA fragment of the *DsRed-Pbcsp* gene was amplified from pDsRed-monomer-N1 (Clontech Laboratories Inc., Mountain View, CA, USA) using primers pDsRed-mono-F1: 5′-CACCGAATTCATG GACAACACCGAGGACGTCATCAAGGA-3′ and pPbCSP-mDsRed-R1: 5′-GCATGCCTAGTCATTTGCGTTTGGTGGTGCT GGGTCATTTGGGTTTGGTGGTGGTGGGTCATTTGCGTTTGG TGGTGGTGGCTGGGAGCCGGAGTGGCGGGCCTCGGCGTG CTCGTACTGCTCCACCACGGT-3′. The PCR product was cloned into pENTR/D-TOPO (Invitrogen, Carlsbad, CA, USA) to generate pENTR-DsRed-Pbcsp. *DsRed-Pbcsp* gene fragment was excised from pENTR-DsRed-Pbcsp by digestion with *Eco*RI and *Sph*I, then cloned into the *Eco*RI/*Sph*I sites of pENTR-aappP-mDsRed-SP15-antryp1T (Yamamoto *et al.*, 2010) to generate pENTR-aappP-mDsRed-Pbcsp-antryp1T. The transformation plasmid pMinos-EGFP-aappP-mDsRed-Pbcsp-antryp1T (Fig. 1A) was generated by incubation of pMinos-EGFP-RfA-F (Yoshida & Watanabe, 2006) and pENTR-aappP-mDsRed-Pbcsp-antryp1T in the presence of LR Clonase (Invitrogen) as described previously (Yoshida & Watanabe, 2006). Procedures for microinjection into embryos, screening of EGFP-expressing G_1 larvae and generation of homozygous lines have been described previously (Catteruccia *et al.*, 2000).

Recombinant protein

A 783-bp DNA fragment of the *P. berghei hsp70* gene (PlasmoDB database, PbANKA_071190) was amplified from *P. berghei* ANKA genomic DNA by PCR using primers phsp70-F1: 5′-CACCGGATCCGAAAGAAATACAACAATCCCAGCTAAAAAA AGCC-3′ and phsp70-R1: 5′-GCGGCCGCATCAACTTCTTCA ACAGTTGGTCCACTTCCAGCTGG-3′. The PCR product was cloned into pENTR-TOPO (Invitrogen) to generate pENTR-PbHSP70. The *hsp70* gene was excised from pENTR-PbHSP70 by digestion with *Bam*HI and *Not*I, and then cloned into the

*Bam*HI/*Not*I sites of pET22-GEX6P2 (Yamamoto *et al.*, 2010) to generate pET22-GEX6P2-HSP70. A recombinant HSP70 protein, created as a fusion protein with glutatione S-transferase (GST), was expressed in *Escherichia coli*. Recombinant HSP70 protein was purified using a Ni-NTA affinity column (Qiagen, Valencia, CA, USA), digested using PreScission protease (GE Healthcare UK Ltd, Buckinghamshire, UK) to remove the GST-tag and fragments were used as antigens for antibody production.

Immunoblotting

Anti-PbCSP antibody (3D11 mAb, MRA-100) was obtained from MR4 (ATCC, Manassas, VA, USA). Rabbit anti-AAPP antiserum was obtained from rabbits immunized with recombinant AAPP protein (Yoshida *et al.*, 2008). Rabbit anti-DsRed polyclonal antibody was purchased from Clontech Laboratories, Inc. Rabbit anti-*P. berghei* HSP70 antiserum was obtained from rabbits immunized with recombinant HSP70 protein.

Groups of 20 pairs of female salivary glands were homogenized using a plastic homogenizer with 40 μl of sample buffer (Nacalai) containing 5% 2-mercaptoethanol, and then boiled at 95 °C for 3 min. The recombinant monomeric DsRed protein was purchased from Clontech Laboratories, Inc., and serially diluted with sample buffer (Nacalai) containing 5% 2-mercaptoethanol, and then boiled at 95 °C for 3 min. Each sample was separated on a 10 or 12% sodium dodecyl sulphate polyacrylamide gel electrophoresis (SDS-PAGE) gel, and transferred to Hybond ECL Membrane (GE Healthcare UK Ltd). The membrane was incubated with 3D11 mAb, anti-AAPP antiserum or anti-DsRed antibody. Polypeptides recognized by the 3D11 mAb were detected with horseradish peroxidase (HRP)-conjugated goat antimouse IgG (H + L) (Bio-rad, Hercules, CA, USA) and polypeptides recognized by either the anti-AAPP antiserum or the anti-DsRed antibody were detected with the HRP-conjugated goat antirabbit IgG (H + L) (Bio-rad). Detection of HRP-labelled antibodies was performed by exposure on a Hyperfilm-ECL (GE Healthcare UK Ltd) using ECL Western Blotting Detection Reagents (GE Healthcare UK Ltd) according to the supplier's protocol. The intensity of bands was analysed using ImageJ software (http://rsbweb.nih.gov/ij/). Groups of 10 female midguts from mosquitoes 15 days after infectious bloodmeal or non-infectious bloodmeal were homogenized using a plastic homogenizer with 100 μl of sample buffer (Nacalai) containing 5% 2-mercaptoethanol, and then boiled at 95 °C for 3 min. Ten μl of each sample (equivalent to one midgut) was separated on a 10% SDS-PAGE gel, and transferred to Hybond ECL Membrane (GE Healthcare UK Ltd). The membrane was incubated with sera from individual mice, 3D11 mAb or rabbit anti-*P. berghei* HSP70 antibody.

Fluorescent microscopy

Following dissection in phosphate-buffered saline (PBS), the female salivary glands were immediately stained with 0.2 mM SYTO-13 (Invitrogen) in PBS for 5 min, and then washed twice with PBS. Fluorescence in the salivary glands was observed using a confocal microscope, FV1000 (Olympus, Tokyo, Japan).

For monitoring salivation with DsRed fluorescence from the proboscis, mosquitoes were kept on ice, their legs and maxillary palps were removed with forceps, and their abdomens were immobilized on a glass slide with adhesion bond. Salivation was observed under a fluorescent microscope BIOREVO (KEYENCE, Osaka, Japan) immediately after immersing the proboscis into 70% glycerol in PBS (Nacalai).

Immunization of mice with TG mosquito bites

ICR mice were used for the analysis of humoral immune responses by mosquito bite. Humoral immune responses against mosquito saliva have been frequently observed using ICR mice (Limesand *et al.*, 2000; Ohtsuka *et al.*, 2001; Thangamani *et al.*, 2010). Moreover, ICR mice were used for the study of mosquito bite *P. berghei* challenge model (Vaughan *et al.*, 1999). DsRed-PbCS3R transgenic or WT female mosquitoes at days 7–10 after emergence were allowed to feed on blood from all over the body of individual mice. To avoid stress and anaemia in the mice, 100 mosquitoes were allowed to bite on mice for 60 min at 1-week intervals. Feeding by mosquitoes was repeated 20 times. Each mouse was subjected to a total of approximately 1500 bites. Sera of the mice that had been bitten by 1500 mosquitoes were subjected to the examination of antibody responses.

ELISA

Sera of the mice repeatedly bitten by either DsRed-Pbcsp or WT mosquitoes were collected individually from the tail vein. PbCSP repeat region peptide (syPbCSP: DPPPNPNDPPPNPND)-specific antibody titres and whole salivary gland protein-specific antibody titres were quantified by ELISA. Groups of 30 pairs of female salivary glands were homogenized using a plastic homogenizer with 300 μl of PBS, and then used for ELISA antigen. Precoated 96-well plates with either syPbCSP at 3 ng/well or the extract of 0.1 pairs of female salivary glands/well in carbonate buffer (15 mM Na_2CO_3, 35 mM $NaHCO_3$, pH 9.6) were incubated with serially diluted sera. Specific total IgGs to each antigen were detected using HRP-conjugated goat antimouse IgG (H + L) (Bio-rad). The plates were developed with a peroxidase substrate solution [H_2O_2 and 2,2′-azino-bis(3-ethylbenzothiazoline-6-sulphonate)]. The optical density at 414 nm of each well was determined using a Multiskan BICHROMATIC microplate reader (Thermo Labsystems, Vantaa, Finland). End-point titres are expressed as the reciprocal of the highest sample dilution for which the optical density was equal to or greater than the mean optical density plus three standard deviations of naive mouse sera.

Immunofluorescence assay

Sporozoites from salivary glands were fixed with 4% paraformaldehyde, washed, blocked with 10% normal goat serum/PBS and incubated with sera from mice repeatedly bitten by mosquitoes (1:100 dilution), followed by antimouse IgG conjugated with Alexa Fluor 594 (Molecular Probes, Carlsbad, CA, USA) or anti-PbCSP 3D11 mAb conjugated with Alexa Fluor 594 (1:200 dilution). Anti-PbCSP 3D11 mAb conjugated with Alexa Fluor 594 was generated using Zenon Antibody Labeling Kits for mouse IgG (Molecular Probes). The specimens were mounted in VECTASHIELD Mounting Media with 4′, 6-diamidino-2-phenylindole (DAPI) (Vector Labs, Inc., Burlingame, CA, USA) observed under a fluorescent microscope, BX51 (Olympus) and a digital camera, DP71 (Olympus).

Cell line

HepG2 cells (American Type Cell Culture, Rockville, MD, USA) were maintained at 37 °C in Dulbecco's modified Eagle's medium (DMEM) (Invitrogen) supplemented with 10% (vol/vol) heat-inactivated foetal bovine serum, 2 mM L-glutamine, 100 U/ml penicillin and 100 μg/ml streptomycin (complete medium).

Sporozoite neutralization assay

HepG2 cells were seeded at a density of 5×10^4 cells/well in 1 ml of DMEM complete medium with a collagen type I-coated 24-well culture plate (BD Biosciences, Franklin Lakes, NJ, USA) 48 h prior to the addition of sporozoites. The sporozoite-neutralization assay was performed as described previously (Kumar *et al.*, 2004). Sporozoites (1×10^4 cells) isolated from the salivary glands of *P. berghei*-infected mosquitoes were incubated with heat-inactivated mouse sera (1:5 dilution) or 50 μg/ml of anti-PbCSP 3D11 mAb. After 72 h of incubation, total RNA was extracted using TRIzol (Invitrogen). Two μg of total RNA was reverse-transcribed from each of the samples using High Capacity cDNA Reverse Transcription kit (Applied Biosystems, Foster City, CA, USA), and cDNA was used for quantitative real-time PCR amplification of *P. berghei 18S rRNA* and HepG2 *beta-actin* gene using Faststart Universal SYBR Green Master (Roche Diagnostics GmbH, Mannheim, Germany). For the amplification of *P. berghei 18S rRNA*, primers Pb18S-F: 5′-GGAGATTGGTTTTGACGTTTATGTG-3′ and Pb18S-R: 5′-AAGCATTAAATAAAGCGAATACATCCTTAC-3′ were used. For the amplification of HepG2 *beta-actin*, primers ACTB-F: 5′-TGGCACCCAGCACAATGAA-3′ and ACTB-R: 5′-CTAAGTCATAGTCCGCCTAGAAGCA-3′ were used. Relative expression of the *P. berghei 18S rRNA* gene was normalized using the *beta-actin* gene of HepG2 cells.

Acknowledgements

We are grateful to J. Sato, K. Watano, H. Okuya, C. Seki, T. Yokomine and K. Yagi for handling of mosquitoes and mice; S. Mizogami (KEYENCE) for fluorescent microscopy technical assistance; Dr K. Sekiné for help with the statistical analysis; and Drs M. Hirai, G.I. Sano, T. Sugo and K. Kasashima for kindly allowing us to use their facilities. This work was supported by grants from the Grand Challenges in Global Health Initiative of Bill and Melinda Gates Foundation to H. M., the Ministry of Education, Culture, Sports and Science of Japan (21390126 to S. Y.) and Jichi Medical University Young Investigator Award to D. S. Y.

References

Alonso, P.L., Sacarlal, J., Aponte, J.J., Leach, A., Macete, E., Milman, J. *et al.* (2004) Efficacy of the RTS,S/AS02A vaccine against *Plasmodium falciparum* infection and disease in young African children: randomised controlled trial. *Lancet* **364**: 1411–1420.

Arca, B., Lombardo, F., Valenzuela, J.G., Francischetti, I.M., Marinotti, O., Coluzzi, M. *et al.* (2005) An updated catalogue of salivary gland transcripts in the adult female mosquito, *Anopheles gambiae*. *J Exp Biol* **208**: 3971–3986.

Bejon, P., Lusingu, J., Olotu, A., Leach, A., Lievens, M., Vekemans, J. *et al.* (2008) Efficacy of RTS,S/AS01E vaccine against malaria in children 5 to 17 months of age. *N Engl J Med* **359**: 2521–2532.

Blandin, S., Moita, L.F., Kocher, T., Wilm, M., Kafatos, F.C. and Levashina, E.A. (2002) Reverse genetics in the mosquito *Anopheles gambiae*: targeted disruption of the *Defensin* gene. *EMBO Rep* **3**: 852–856.

Bonnet, S., Prevot, G., Jacques, J.C., Boudin, C. and Bourgouin, C. (2001) Transcripts of the malaria vector *Anopheles gambiae* that are differentially regulated in the midgut upon exposure to invasive stages of *Plasmodium falciparum*. *Cell Microbiol* **3**: 449–458.

Brown, A.E., Bugeon, L., Crisanti, A. and Catteruccia, F. (2003) Stable and heritable gene silencing in the malaria vector *Anopheles stephensi*. *Nucleic Acids Res* **31**: e85.

Catteruccia, F., Nolan, T., Loukeris, T.G., Blass, C., Savakis, C., Kafatos, F.C. *et al.* (2000) Stable germline transformation of the malaria mosquito *Anopheles stephensi*. *Nature* **405**: 959–962.

Chen, X.G., Mathur, G. and James, A.A. (2008) Gene expression studies in mosquitoes. *Adv Genet* **64**: 19–50.

Cohen, J., Nussenzweig, V., Nussenzweig, R., Vekemans, J. and Leach, A. (2010) From the circumsporozoite protein to the RTS, S/AS candidate vaccine. *Hum Vaccin* **6**: 90–96.

Coppi, A., Natarajan, R., Pradel, G., Bennett, B.L., James, E.R., Roggero, M.A. *et al.* (2011) The malaria circumsporozoite protein has two functional domains, each with distinct roles as sporozoites journey from mosquito to mammalian host. *J Exp Med* **208**: 341–356.

Crampton, J.M., Stowell, S.L., Karras, M. and Sinden, R.E. (1999) Model systems to evaluate the use of transgenic haematophagous insects to deliver protective vaccines. *Parassitologia* **41**: 473–477.

Egan, J.E., Weber, J.L., Ballou, W.R., Hollingdale, M.R., Majarian, W.R., Gordon, D.M. *et al.* (1987) Efficacy of murine malaria sporozoite vaccines: implications for human vaccine development. *Science* **236**: 453–456.

Francischetti, I.M., Valenzuela, J.G., Pham, V.M., Garfield, M.K. and Ribeiro, J.M. (2002) Toward a catalog for the transcripts and proteins (sialome) from the salivary gland of the malaria vector Anopheles gambiae. *J Exp Biol* **205**: 2429–2451.

Handler, A.M. and O'Brochta, D.A. (2009) Transposable element for insect transformation. In *Insect Development: Morphogenesis, Molting Metamorphosis* (Gilbert, L.I., ed.), pp. 459–496. Academic Press, London.

Harada, M., Ikeshoji, T. and Suguri, S. (1998) Studies on vector control by 'Mosquito Candle'. In *Malaria Research in the Solomon Island* (Ishii, A., Nihei, N. and Sasa, M., eds), pp. 120–125. Inter Group Corporation, Tokyo.

Hii, J.L., Kanai, L., Foligela, A., Kan, S.K., Burkot, T.R. and Wirtz, R.A. (1993) Impact of permethrin-impregnated mosquito nets compared with DDT house-spraying against malaria transmission by *Anopheles farauti* and *An. punctulatus* in the Solomon Islands. *Med Vet Entomol* **7**: 333–338.

Hollingdale, M.R., Nardin, E.H., Tharavanij, S., Schwartz, A.L. and Nussenzweig, R.S. (1984) Inhibition of entry of *Plasmodium falciparum* and *P. vivax* sporozoites into cultured cells; an *in vitro* assay of protective antibodies. *J Immunol* **132**: 909–913.

Holt, R.A., Subramanian, G.M., Halpern, A., Sutton, G.G., Charlab, R., Nusskern, D.R. *et al.* (2002) The genome sequence of the malaria mosquito *Anopheles gambiae*. *Science* **298**: 129–149.

Isaacs, A.T., Li, F., Jasinskiene, N., Chen, X., Nirmala, X., Marinotti, O. *et al.* (2011) Engineered resistance to *Plasmodium falciparum* development in transgenic *Anopheles stephensi*. *PLoS Pathog* **7**: e1002017.

Ito, J., Ghosh, A., Moreira, L.A., Wimmer, E.A. and Jacobs-Lorena, M. (2002) Transgenic anopheline mosquitoes impaired in transmission of a malaria parasite. *Nature* **417**: 452–455.

Kost, T.A., Condreay, J.P. and Jarvis, D.L. (2005) Baculovirus as versatile vectors for protein expression in insect and mammalian cells. *Nat Biotechnol* **23**: 567–575.

Kumar, K.A., Oliveira, G.A., Edelman, R., Nardin, E. and Nussenzweig, V. (2004) Quantitative *Plasmodium* sporozoite neutralization assay (TSNA). *J Immunol Methods* **292**: 157–164.

Limesand, K.H., Higgs, S., Pearson, L.D. and Beaty, B.J. (2000) Potentiation of vesicular stomatitis New Jersey virus infection in mice by mosquito saliva. *Parasite Immunol* **22**: 461–467.

Mathur, G., Sanchez-Vargas, I., Alvarez, D., Olson, K.E., Marinotti, O. and James, A.A. (2010) Transgene-mediated suppression of dengue viruses in the salivary glands of the yellow fever mosquito, *Aedes aegypti*. *Insect Mol Biol* **19**: 753–763.

Matsuoka, H., Ikezawa, T. and Hirai, M. (2010) Production of a transgenic mosquito expressing circumsporozoite protein, a malarial protein, in the salivary gland of *Anopheles stephensi* (Diptera: Culicidae). *Acta Med Okayama* **64**: 233–241.

Nene, V., Wortman, J.R., Lawson, D., Haas, B., Kodira, C., Tu, Z.J. *et al.* (2007) Genome sequence of *Aedes aegypti*, a major arbovirus vector. *Science* **316**: 1718–1723.

Ohtsuka, E., Kawai, S., Ichikawa, T., Nojima, H., Kitagawa, K., Shirai, Y. *et al.* (2001) Roles of mast cells and histamine in mosquito bite-induced allergic itch-associated responses in mice. *Jpn J Pharmacol* **86**: 97–105.

Ribeiro, J.M., Arca, B., Lombardo, F., Calvo, E., Phan, V.M., Chandra, P.K. *et al.* (2007) An annotated catalogue of salivary gland transcripts in the adult female mosquito, *Aedes aegypti*. *BMC Genomics* **8**: 6.

Ribeiro, J.M., Mans, B.J. and Arca, B. (2010) An insight into the sialome of blood-feeding Nematocera. *Insect Biochem Mol Biol* **40**: 767–784.

Rodrigues, F.G., Santos, M.N., de Carvalho, T.X., Rocha, B.C., Riehle, M.A., Pimenta, P.F. *et al.* (2008) Expression of a mutated phospholipase A2 in transgenic *Aedes fluviatilis* mosquitoes impacts *Plasmodium gallinaceum* development. *Insect Mol Biol* **17**: 175–183.

Sanders, H.R., Evans, A.M., Ross, L.S. and Gill, S.S. (2003) Blood meal induces global changes in midgut gene expression in the disease vector, *Aedes aegypti*. *Insect Biochem Mol Biol* **33**: 1105–1122.

Tam, J.P., Clavijo, P., Lu, Y.A., Nussenzweig, V., Nussenzweig, R. and Zavala, F. (1990) Incorporation of T and B epitopes of the circumsporozoite protein in a chemically defined synthetic vaccine against malaria. *J Exp Med* **171**: 299–306.

Terenius, O., Marinotti, O., Sieglaff, D. and James, A.A. (2008) Molecular genetic manipulation of vector mosquitoes. *Cell Host Microbe* **4**: 417–423.

Thangamani, S., Higgs, S., Ziegler, S., Vanlandingham, D., Tesh, R. and Wikel, S. (2010) Host immune response to mosquito-transmitted chikungunya virus differs from that elicited by needle inoculated virus. *PLoS ONE* **5**: e12137.

Thathy, V., Fujioka, H., Gantt, S., Nussenzweig, R., Nussenzweig, V. and Menard, R. (2002) Levels of circumsporozoite protein in the *Plasmodium* oocyst determine sporozoite morphology. *EMBO J* **21**: 1586–1596.

Tomita, M. (2011) Transgenic silkworms that weave recombinant proteins into silk cocoons. *Biotechnol Lett* **33**: 645–654.

Valenzuela, J.G., Francischetti, I.M., Pham, V.M., Garfield, M.K. and Ribeiro, J.M. (2003) Exploring the salivary gland transcriptome and proteome of the *Anopheles stephensi* mosquito. *Insect Biochem Mol Biol* **33**: 717–732.

Vaughan, J.A., Scheller, L.F., Wirtz, R.A. and Azad, A.F. (1999) Infectivity of Plasmodium berghei sporozoites delivered by intravenous inoculation versus mosquito bite: implications for sporozoite vaccine trials. *Infect Immun* **67**: 4285–4289.

Waitayakul, A., Somsri, S., Sattabongkot, J., Looareesuwan, S., Cui, L. and Udomsangpetch, R. (2006) Natural human humoral response to salivary gland proteins of *Anopheles* mosquitoes in Thailand. *Acta Trop* **98**: 66–73.

Wang, R., Charoenvit, Y., Corradin, G., Porrozzi, R., Hunter, R.L., Glenn, G. *et al.* (1995) Induction of protective polyclonal antibodies by immunization with a *Plasmodium yoelii* circumsporozoite protein multiple antigen peptide vaccine. *J Immunol* **154**: 2784–2793.

Yamamoto, D.S., Nagumo, H. and Yoshida, S. (2010) Flying vaccinator; a transgenic mosquito delivers a *Leishmania* vaccine via blood feeding. *Insect Mol Biol* **19**: 391–398.

Yoshida, N., Potocnjak, P., Nussenzweig, V. and Nussenzweig, R.S. (1981) Biosynthesis of Pb44, the protective antigen of sporozoites of Plasmodium berghei. *J Exp Med* **154**: 1225–1236.

Yoshida, S. and Watanabe, H. (2006) Robust salivary gland-specific transgene expression in *Anopheles stephensi* mosquito. *Insect Mol Biol* **15**: 403–410.

Yoshida, S., Shimada, Y., Kondoh, D., Kouzuma, Y., Ghosh, A.K., Jacobs-Lorena, M. *et al.* (2007) Hemolytic C-type lectin CEL-III from sea cucumber expressed in transgenic mosquitoes impairs malaria parasite development. *PLoS Pathog* **3**: e192.

Yoshida, S., Sudo, T., Niimi, M., Tao, L., Sun, B., Kambayashi, J. *et al.* (2008) Inhibition of collagen-induced platelet aggregation by anopheline antiplatelet protein, a saliva protein from a malaria vector mosquito. *Blood* **111**: 2007–2014.

Yoshida, S., Kawasaki, M., Hariguchi, N., Hirota, K. and Matsumoto, M. (2009) A baculovirus dual expression system-based malaria vaccine induces strong protection against *Plasmodium berghei* sporozoite challenge in mice. *Infect Immun* **77**: 1782–1789.

Yoshida, S., Araki, H. and Yokomine, T. (2010a) Baculovirus-based nasal drop vaccine confers complete protection against malaria by natural boosting of vaccine-induced antibodies in mice. *Infect Immun* **78**: 595–602.

Yoshida, S., Nagumo, H., Yokomine, T., Araki, H., Suzuki, A. and Matsuoka, H. (2010b) *Plasmodium berghei* circumvents immune responses induced by merozoite surface protein 1- and apical membrane antigen 1-based vaccines. *PLoS ONE* **5**: e13727.

Zavala, F., Tam, J.P., Barr, P.J., Romero, P.J., Ley, V., Nussenzweig, R.S. *et al.* (1987) Synthetic peptide vaccine confers protection against murine malaria. *J Exp Med* **166**: 1591–1596.

Supporting Information

Additional Supporting Information may be found in the online version of this article under the DOI reference: 10.1111/j.1365-2583.2011.01128.x

Figure S1. Structure of the mDsRed gene and Southern blot analysis of the DsRed-PbCS3R mosquito. (A) Schematic representation of genomic structure of the DsRed-PbCS3R mosquito. ITR, *Minos* inverted terminal repeat; *actin*P, *Drosophila melanogaster actin5c* promoter; *egfp*, enhanced green fluorescent protein-coding sequence; *hsp*T, *D. melanogaster* terminator sequence; *aapp*P, *Anopheles stephensi anopheline antiplatelet protein* promoter; *mDsRed*, monomeric DsRed-coding sequence; PbCS3R, three tandemly repeated unit region of *Plasmodium berghei* circumsporozoite protein-coding sequence; trypT, *Anopheles gambiae trypsin* terminator sequence. A black bar represents the probe region used for Southern blot analysis. (B) Southern blot analysis of the DsRed-PbCS3R mosquito. Genomic DNAs from four independent DsRed-PbCS3R transgenic lines were digested with *Bam*HI, and hybridized with a 0.7 kb DNA fragment encoding the monomeric DsRed protein. Leftmost lane shows size markers (kb).

Figure S2. Percentage sporozoite inhibition associated with sera from mice repeatedly bitten by transgenic mosquitoes and wild-type (WT) mosquitoes using the sporozoite-neutralization assay. The sporozoite-neutralization assay was performed using sera from mice repeatedly bitten by DsRed-PbCS3R mosquitoes (no. 2) or WT mosquitoes (no. 6). Twenty-five μg/μl of 3D11 mouse monoclonal antibody (mAb) and naïve mouse sera were used as a positive control and a negative control, respectively. The relative level of *Plasmodium berghei* sporozoite 18S rRNA with naïve mouse serum was defined as 100%. Quantitative real-time PCR was performed three times using the templates. The p-value between the two groups was calculated by Welch's two sample *t*-test with Bonferroni correction. *, $P < 0.001$; n.s., not significant. Percentage inhibition values have been indicated at the top of each bar. Percentage inhibition values were obtained using the following formula: 100-[relative level of *P. berghei* sporozoite *18S rRNA* (%)]. N.I., no inhibition.

Please note: Neither the Editors nor Wiley-Blackwell are responsible for the content or functionality of any supporting materials supplied by the authors. Any queries (other than missing material) should be directed to the corresponding author for the article.

European Journal of Immunology

A critical role for phagocytosis in resistance to malaria in iron-deficient mice

Chikako Matsuzaki-Moriya[1], Liping Tu[1], Hidekazu Ishida[2], Takashi Imai[2], Kazutomo Suzue[2], Makoto Hirai[2], Kohhei Tetsutani[1], Shinjiro Hamano[1], Chikako Shimokawa[1] and Hajime Hisaeda[2]

[1] Department of Microbiology and Immunology, Graduate School of Medical Sciences, Kyushu University, Fukuoka, Japan
[2] Department of Parasitology, Graduate School of Medicine, Gunma University, Maebashi, Japan

Both iron-deficient anemia (IDA) and malaria remain a threat to children in developing countries. Children with IDA are resistant to malaria, but the reasons for this are unknown. In this study, we addressed the mechanisms underlying the protection against malaria observed in IDA individuals using a rodent malaria parasite, *Plasmodium yoelii* (Py). We showed that the intra-erythrocytic proliferation and amplification of Py parasites were not suppressed in IDA erythrocytes and immune responses specific for Py parasites were not enhanced in IDA mice. We also found that parasitized IDA cells were more susceptible to engulfment by phagocytes in vitro than control cells, resulting in rapid clearance of parasitized cells and that protection of IDA mice from malaria was abrogated by inhibiting phagocytosis. One possible reason for this rapid clearance might be increased exposure of phosphatidylserine at the outer leaflet of parasitized IDA erythrocytes. The results of this study suggest that parasitized IDA erythrocytes are eliminated by phagocytic cells, which sense alterations in the membrane structure of parasitized IDA erythrocytes.

Key words: Iron-deficient anemia · Macrophages · Malaria · Phosphatidylserine

Introduction

Iron deficiency is the most common and widespread nutritional disorder in the world. In many disorders resulting from a lack of iron, hemoglobin synthesis is deeply suppressed, resulting in iron-deficient anemia (IDA). IDA is characterized by small erythrocytes (microcytic) that contain less hemoglobin (hypochromic). IDA is mainly caused by a low dietary intake of iron, but can also be caused by chronic intestinal hemorrhage associated with hookworm infestation or by vitamin A deficiency, which is critical for iron metabolism. Both are common in developing countries [1]. Nearly half of the children living in developing countries are estimated to suffer from IDA; twice the number in industrialized countries. Iron deficiency adversely affects cognitive performance, behavior and physical growth, and IDA patients experience impaired gastrointestinal function and altered patterns of hormone production and metabolism [1]. Moreover, morbidity due to infectious diseases is increased in iron-deficient populations because of its adverse effects on the immune system [1, 2]. Based on this, the World Health Organization recommends iron supplementation for children and pregnant women to treat IDA.

Malaria is still a major health problem, resulting in more than 200 million infections and around a million deaths annually [3]. Almost all victims of malaria are children under 5 years of age living in sub-Saharan Africa [3], whose geographical and age distribution completely overlap those of IDA. Thus, the coexistence of IDA and malaria seems common, and IDA may modulate the course of malaria. In Kenya, however, clinical malaria is significantly less frequent among iron-deficient

Correspondence: Dr. Hajime Hisaeda
e-mail: hisa@med.gunma-u.ac.jp

children [4]. In infants from Papua New Guinea, iron supplementation increased the prevalence of parasitemia [5]. In the largest study, involving Zanzibari children, routine supplementation with iron and folate was found to increase the risk of severe malaria and death [6]. Taken together, these findings suggest that routine supplementation with iron, or iron plus folate, increases childhood morbidity and mortality from malaria. Recently, one study assessed the effect of iron supplementation on the intermittent preventive treatment of malaria [7]; however, the mechanisms involved are still not fully understood.

Here, we addressed the mechanisms underlying decreased susceptibility to malaria in IDA individuals using a mouse malaria model. We found that macrophages preferentially sensed and engulfed parasitized erythrocytes from IDA mice, resulting in rapid clearance of the parasite from the circulation. One possible reason for this rapid clearance may be increased phosphatidylserine (PS) exposure at the outer leaflet of parasitized IDA erythrocytes.

Results

Induction of IDA

C57BL/6 mice were fed with a chemically defined iron-deficient diet to mimic IDA, the most prevalent form of anemia observed in endemic areas of malaria. The effect of this diet on hematopoiesis was assessed by measuring a number of hematological variables (Table 1). Ten weeks of an iron-deficient diet resulted in decreased erythrocyte and hemoglobin concentrations. The MCV (mean corpuscular volume, volume per individual erythrocyte) was also reduced in these mice, confirming the successful induction of IDA characterized by microcytic anemia.

Mice with IDA are protected from early death due to malaria

Iron-deficient mice were infected with *Plasmodium yoelii* (Py) and the kinetics of infection assessed by evaluating the daily levels of parasitemia and survival rates. Py has two substrains, PyL and PyNL, each with differing virulence. Infection of iron-sufficient mice with the virulent strain, PyL, resulted in a rapid increase in parasitemia that killed all mice within 10 days (Fig. 1A). Interestingly, IDA mice showed markedly lower levels of parasitemia throughout the period of infection and survived longer than iron-sufficient control mice. They finally succumbed to infection with low levels of parasitemia, presumably due to severe anemia (Fig. 1A). Mice infected with LD_{50} of the PyNL strain (less virulent than PyL) experienced peak levels of parasitemia 3 wk after infection followed by complete eradication of the parasites. Mice cured of PyNL infection showed sterile immunity against otherwise-lethal infections by PyL [8]. IDA mice had low levels of parasitemia and all of them survived (Fig. 1B). A detailed evaluation showed that the numbers of late trophozoites and shizonts were significantly reduced (Fig. 1C). These results clearly demonstrated that IDA mice were protected from death caused by acute Py infection. This protection was not limited to infection with Py, as similar results were obtained when IDA mice were infected with the *P. berghei* NK65 strain (data not shown).

Table 1. Hematological variables in mice after 10-wk feeding with iron-deficient diet

	Control	ID
Hematocrit (%)	50.0±0.82*	34.3±0.47
Hemoglobin (g/dL)	12.3±0.35*	8.0±0.40
RBC count (10^4/cmm)	911.7±44.97*	731.0±41.70
MCV (fl)	55.0±2.51*	47.1±3.04
MCH (pg)	24.7±0.90	23.2±0.84
MCHC (g/dL)	13.6±1.07	10.93±1.03

Each value represents mean±SD from six mice. Asterisks indicate significant difference between control and ID group. MCV: mean corpuscular volume; MCH: mean corpuscular hemoglobin; MCHC: mean corpuscular hemoglobin concentration.

IDA has no effect on parasite growth

To address the mechanisms underlying resistance to malaria in IDA, two possibilities were raised. One relates to the direct effects on the parasites themselves; the development/growth of the parasites is suppressed in IDA erythrocytes. The other is that iron-deficiency modulates host immunity to enhance the eradication of parasites. We first focused on the intra-erythrocytic development of the malaria parasites. Erythrocytes isolated from IDA mice during the early phase of PyL infection were cultured in the presence of 10% normal mouse serum and periodically observed under a microscope. The purified infected cells were almost ring-infected and developed into late trophozoites within 3 h. They developed into mature schizonts after nuclear division within 6 h. PyL parasites grew equally well in IDA erythrocytes and control erythrocytes (Fig. 2A). To further mimic the in vivo situation, we used serum from IDA mice. Under these conditions the parasites still grew in the presence of IDA serum (Fig. 2A). Furthermore, we did not observe any differences in the number of merozoites within the individual mature schizonts in vivo (Fig. 2B). These results seem to exclude the possibility that IDA adversely affects the development/growth of malaria parasites.

Acquired immunity is not involved in resistance of IDA mice to malaria

We next analyzed the effects of IDA on host immunity. Our previous reports showed that infection with PyL, but not PyNL, activates Tregs, indicating that the virulence of Py is determined by immunosuppression associated with Treg activation [9]. Activation of Tregs during infection with PyL requires TLR9 signaling in DCs

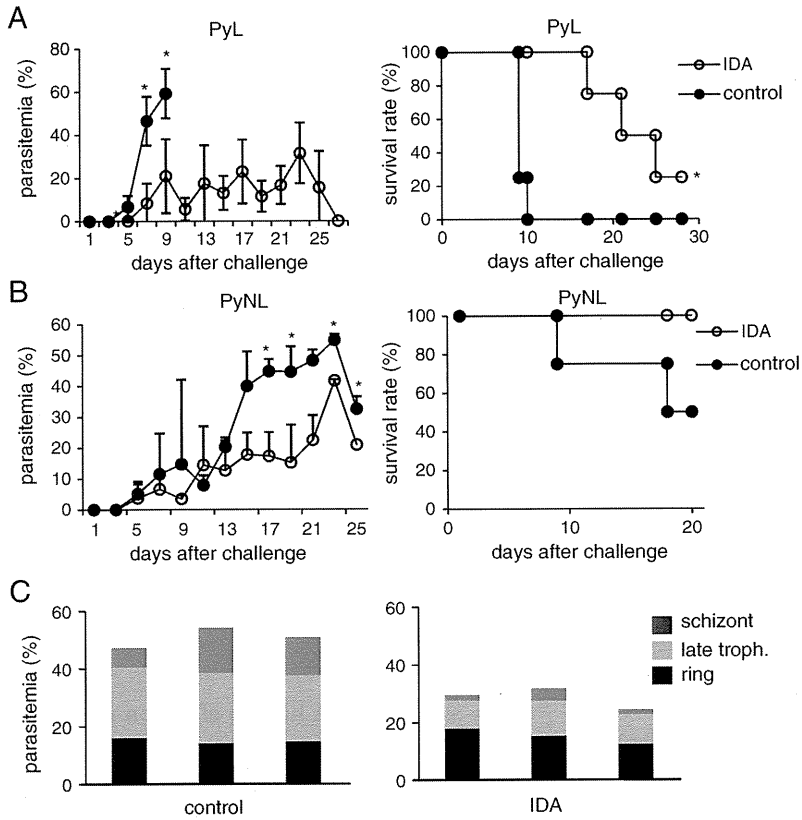

Figure 1. Protection against Py in IDA mice. Percentage parasitemia (left panels) and survival rates (right panels) in mice infected with (A) PyL or (B) PyNL. Data are presented as the mean parasitemia ± SD (from six mice). In the left panels, asterisks represent significant differences ($p<0.05$) in parasitemia (%) between IDA and control mice. In the right panels, asterisks indicate statistical significance ($p<0.05$) using the Breslow-Gehan-Wilcon test of the Kaplan–Meier method between IDA and control mice. (C) Parasitemia during each erythrocytic stage in mice infected with PyL. The results from three individual mice obtained 6 days after infection are shown. Four repeated experiments showed similar results.

[10]. It is quite possible that Tregs are not activated in IDA mice due to insufficient TLR9 signaling because IDA erythrocytes contain much less hemoglobin/heme (data not shown), the source of a known malaria-derived TLR9 ligand, hemozoin [11]. Thus, we analyzed the immune responses in IDA mice. First, we assessed the number of cells involved in protection against malaria in the spleen 6 days after infection with PyL (Fig. 3A). Infection with PyL clearly increased the population of spleen cells. Unexpectedly, the number of whole splenocytes and splenic $CD4^+CD25^-$ T cells in IDA mice was less than that in control mice. There was no increase in the number of macrophages.

IFN-γ production by whole spleen cells in response to ConA was evaluated using ELISA. Infection of control mice with PyL markedly reduced the production of IFN-γ; however, infection of IDA mice reduced it to an even greater degree (Fig. 3B). The production of IgG antibodies specific for the malaria parasite was also assessed. Humoral immunity to the malaria parasite was induced after infection with PyL in iron-sufficient mice. However, IDA mice had much lower total IgG levels (Fig. 3C). Thus, neither humoral nor cellular responses were enhanced in IDA mice.

We further evaluated the functional properties of splenic Tregs by investigating the suppression of TCR-driven T-cell proliferation. $CD4^+CD25^+$ T cells isolated from IDA mice were cultured with $CD4^+CD25^-$ T cells from uninfected mice in the presence of ConA. Tregs from uninfected mice suppressed proliferation in a dose-dependent manner. Infection of iron-sufficient mice with PyL markedly enhanced the suppressive function of Tregs, reflecting Treg activation (Fig. 3D). Tregs in IDA mice had much stronger suppressive abilities (Fig. 3D), presumably resulting in reduced immune responses in these mice. Again, we saw no evidence for the enhancement of acquired immunity in IDA mice.

Finally, to analyze whether acquired immunity is involved in the resistance of IDA mice to malaria, we infected T-cell and iron-deficient athymic nude mice with PyL. As shown previously, IDA euthymic mice showed lower levels of parasitemia and prolonged survival compared with euthymic mice fed with an iron-sufficient diet (Fig. 3E). IDA athymic mice clearly showed lower levels of parasitemia than mice fed with an iron-sufficient diet although they still succumbed to infection with PyL. These results suggest that acquired immunity, in which T cells play a central role, is required to survive infection by PyL, but it is not involved in IDA-associated resistance to malaria during the early phase of infection.

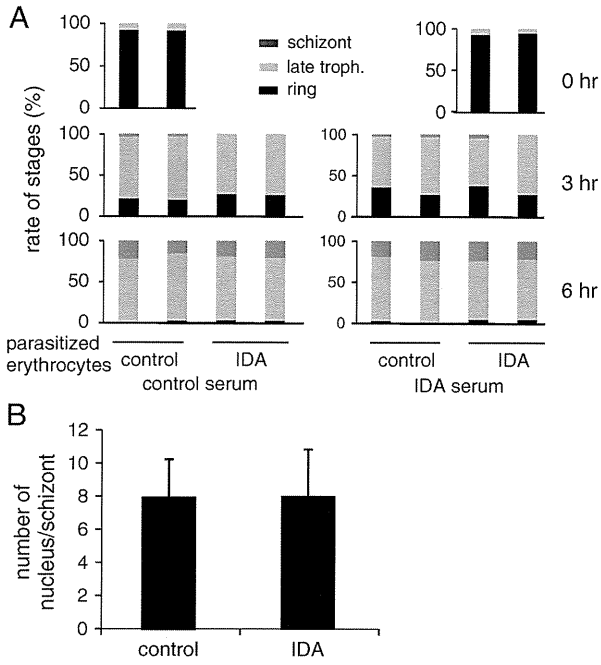

Figure 2. Intra-erythrocytic development and amplification of PyL in IDA erythrocytes. (A) Erythrocytes infected with the ring form of PyL from IDA mice were cultured in the presence control serum (left panels) or serum from IDA mice (left panels) and the developmental stages assessed microscopically after the indicated culture periods. The ratio of erythrocytes infected with ring form, late trophozoite, and schizonts to the total number of erythrocytes infected with asexual parasites is shown. Three individual mice were used in each group. (B) The number of merozoites in schizont-infected erythrocytes in whole blood obtained from IDA mice was counted under a microscope. Blood smears were prepared on 7, 9, and 11 days after challenge. Data represent the means ± SD from 150 schizonts. Three repeated experiments showed similar results.

Enhanced phagocytosis of IDA erythrocytes infected with Py

Considering the resistance observed in IDA mice during the very early phase of infection, innate immunity and/or more primitive protective mechanisms might be operating. One of the first lines of defense against blood-stage malaria is phagocytosis followed by digestion of parasitized erythrocytes by phagocytic cells [12]. To examine the possibility that the phagocytic ability of macrophages is involved in resistance, peritoneal macrophages obtained from IDA mice were cultured with CFSE-labeled parasitized erythrocytes purified from PyL-infected iron-sufficient mice and analyzed for their phagocytic ability. Macrophages from both iron-sufficient and iron-deficient mice phagocytosed parasitized erythrocytes, but not uninfected erythrocytes (Fig. 4A). Activation of phagocytes in IDA mice could not explain this phenomenon.

Previous reports showed that parasitized IDA erythrocytes are engulfed by phagocytic cells [13]. Therefore, we assessed the difference in susceptibility to phagocytosis between IDA and control parasitized erythrocytes. Percoll-purified schizonts from IDA mice infected with PyL were labeled with CFSE and cultured with peritoneal macrophages obtained from control mice. As shown previously, a small population of $CD11b^+$ macrophages ingested parasitized erythrocytes from iron-sufficient mice (Fig. 4B). Surprisingly, almost all macrophages phagocytosed parasitized IDA erythrocytes. $CD11b^+$ macrophages contained higher levels of CFSE, suggesting engulfment of multiple parasitized erythrocytes (Fig. 4B). This enhanced susceptibility to phagocytosis was limited to parasitized cells, as macrophages did not ingest erythrocytes from uninfected IDA mice (Fig. 4B). Similar results were obtained using macrophages isolated from the spleen, in which the malarial parasites encounter host immune cells (Fig. 4C). To further analyze these observations in vivo, we intravenously inoculated uninfected mice with CFSE-labeled parasitized IDA erythrocytes and examined their clearance from the circulation. Uninfected erythrocytes were constantly detected throughout the entire course of the experiment (Fig. 4D). Consistent with the in vitro studies, purified schizonts from IDA mice were more rapidly eliminated from the circulation than those from control mice (Fig. 4D). This was more obvious when purified ring-infected erythrocytes were used. The clearance of ring-infected erythrocytes from IDA mice was comparable to that of schizonts, whereas ring-infected iron-sufficient erythrocytes were retained for up to 60 min (Fig. 4D). $F4/80^+$ red pulp macrophages may be responsible for phagocytosis of IDA parasitized erythrocytes in vivo (Fig. 4E).

The rapid clearance of parasitized IDA erythrocytes is due to the enhanced ability of phagocytic cells to capture them. Mice treated with carrageenan (CGN), which impairs the function of phagocytic cells, showed a significant delay in the elimination of IDA schizonts. In contrast, iron-sufficient schizonts were eliminated regardless of whether they were treated with CGN (Fig. 5A). Finally, we evaluated the contribution of enhanced phagocytosis of parasitized IDA erythrocytes to the resistance of IDA mice to malaria. Treatment with CGN completely reversed the lower levels of parasitemia and prolonged survival of IDA mice infected with PyL, but did not alter the course of infection in iron-sufficient mice (Fig. 5B). These results indicate that phagocytosis of parasitized IDA cells plays a critical role in resistance to malaria in IDA mice.

PS exposure in IDA parasitized erythrocytes

We next explored the mechanisms underlying the enhanced phagocytosis specific for parasitized IDA erythrocytes by focusing on alterations in the membrane structure, especially the increased exposure of PS, which is usually located within the inner leaflet of the lipid bilayer. Exposure of PS is one of the hallmarks of apoptotic nucleated cells and provides an "eat me" signal to phagocytic cells, resulting in rapid clearance of apoptotic cells without any inflammatory consequences. PS-dependent phagocytosis is involved in the physiological clearance of erythrocytes after their natural lifespan [14]; therefore, we estimated the levels of PS exposure in IDA mice

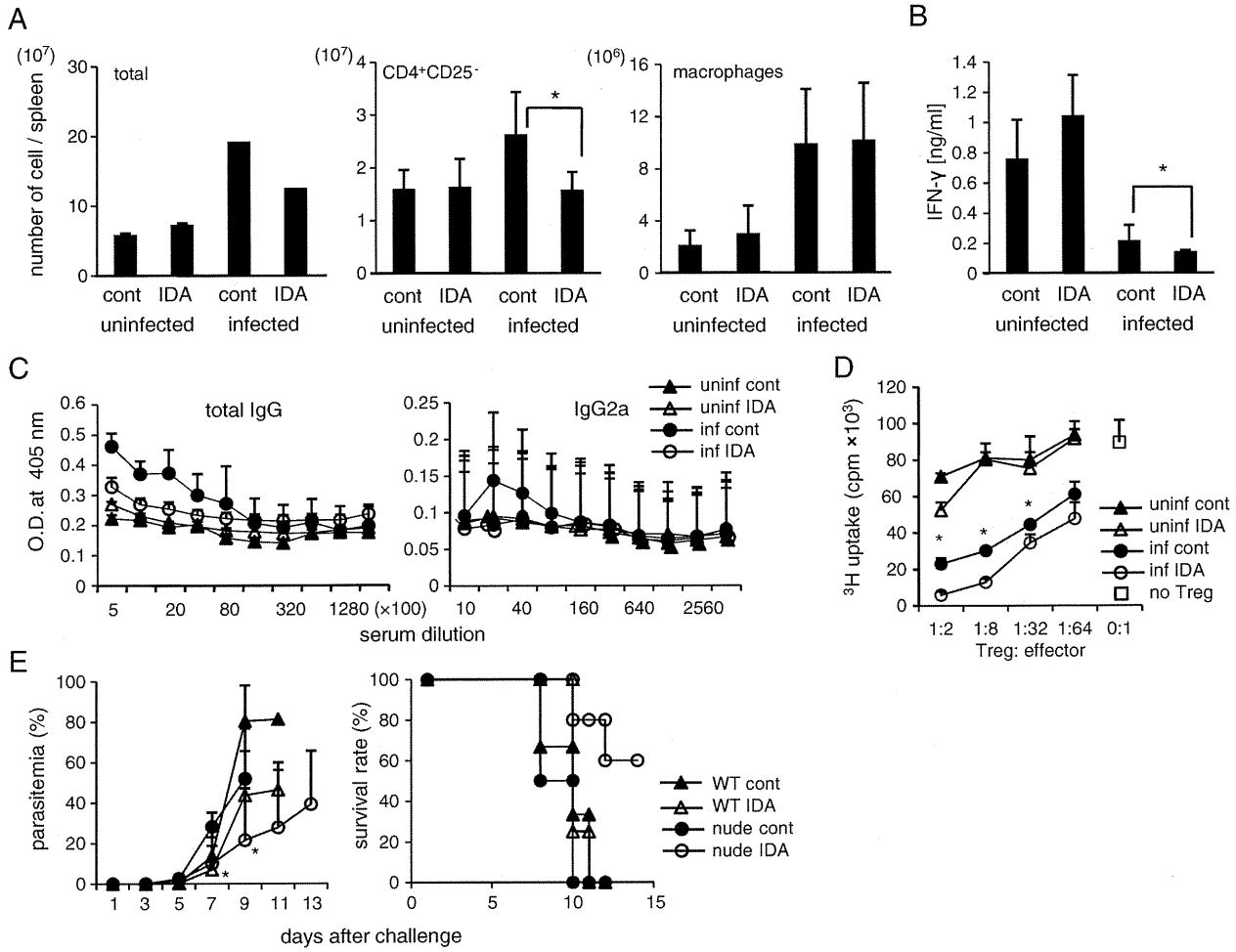

Figure 3. Effects of IDA on acquired immunity in mice infected with Py. Spleen cells obtained 6 days after infection by PyL were analyzed for (A) the number of the indicated cells and for (B) IFN-γ production after 48 h of culture with ConA. Data represent the mean ± SD from 6 mice (A) or 3 mice (B). *$p<0.05$. (C) Sera were obtained from the indicated mice 7 days after infection. Antibodies specific for parasite antigens were analyzed by ELISA. The vertical and horizontal axes represent OD at 405 nm and the dilution factor, respectively. Results represent the mean ± SD of triplicate wells. Each group contained three mice. (D) To examine the suppressive function of $CD4^+CD25^+$ cells after PyL infection, $CD4^+CD25^-$ T cells (2×10^5) purified from uninfected mice were stimulated with ConA and APC in the presence of $CD25^+$ T cells from uninfected controls (filled triangles), uninfected IDA (open triangles), infected controls (filled circles) and infected IDA (open circles) mice 5 days after infection at the indicated ratio to $CD4^+CD25^-$ T cells. Asterisks denote significant differences ($p<0.05$) in ^{3}[H]-thymidine uptake (cpm) between infected controls and infected IDA groups. (E) To assess the effects of IDA on susceptibility of T-cell-deficient nude mice, we infected the indicated mice with PyL and monitored parasitemia and survival rate. Values for parasitemia are arithmetic means ± SD from six mice in each group. *$p<0.05$, in parasitemia between iron-sufficient and IDA WT mice and between iron-sufficient and IDA nude mice 7 and 9 days after infection, respectively (left panel). Two repeated experiments showed similar results.

infected by PyL using flow cytometry to analyze the binding of annexin V. Peripheral blood was stained with an anti-CD71 (transferrin receptor) antibody and Syto 16, which binds to nucleic acids, to distinguish parasitized erythrocytes from reticulocytes, which are increased in IDA mice. Syto 16 stained both parasite-derived nucleic acids and the residual RNA in reticulocytes. Because PyL invades mature erythrocytes – but not reticulocytes – expressing CD71 [15], Syto 16^+ cells within the $CD71^-$ mature erythrocytes represented parasitized erythrocytes. The percentage of annexin V-binding parasitized erythrocytes in the IDA mice was markedly increased compared with that in the control mice (Fig. 6), suggesting that increased exposure of PS resulted in higher susceptibility of IDA erythrocytes to phagocytosis. It should be noted that a substantial fraction of uninfected erythrocytes bound annexin V, suggesting that infection may have an effect on membrane remodeling in uninfected as well as in infected cells.

Cytosolic Ca^{2+} concentration increases in IDA erythrocytes after infection with PyL

Finally, we analyzed the putative mechanisms underlying PS exposure in parasitized IDA erythrocytes. The enzymes

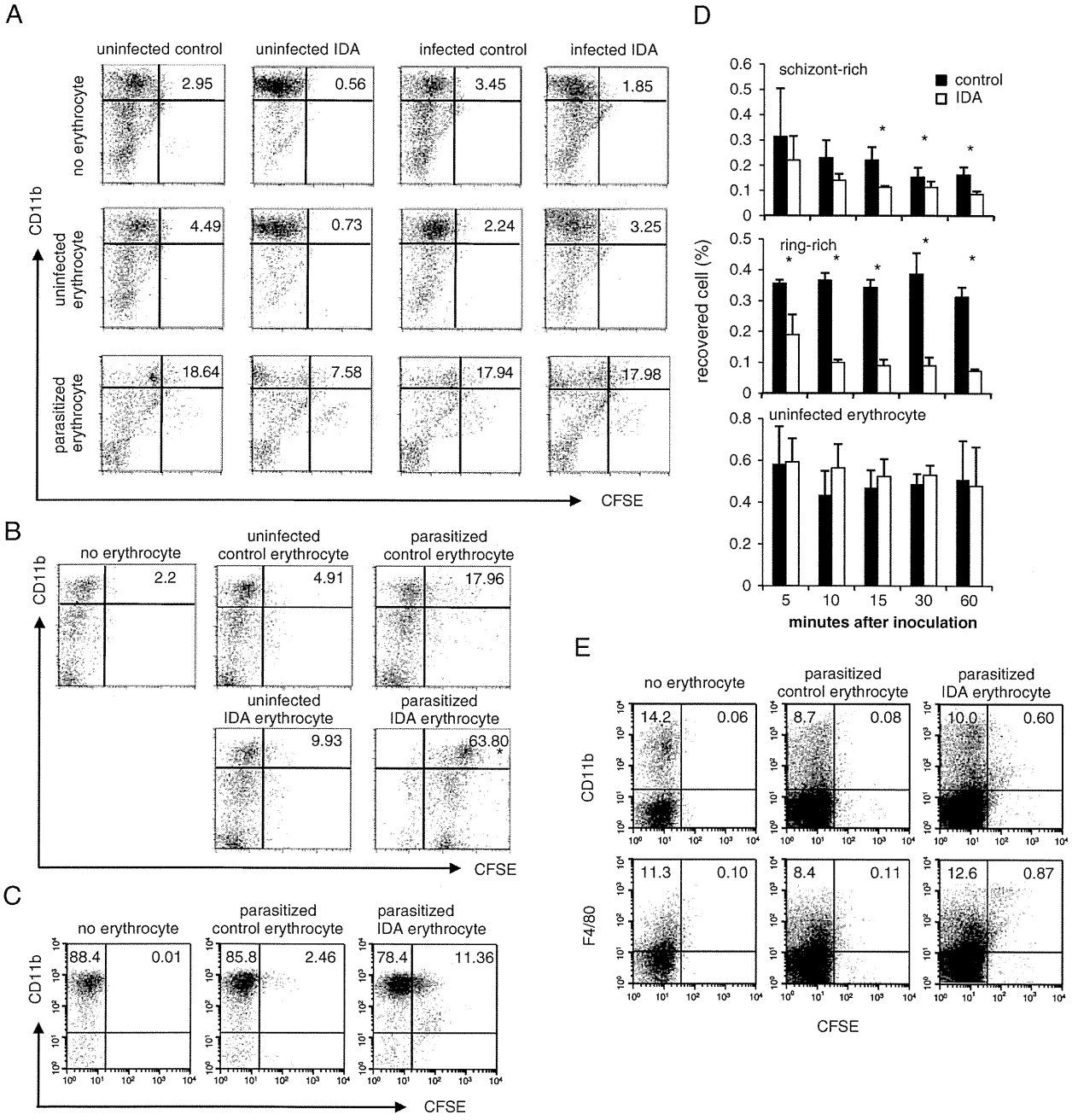

Figure 4. Rapid clearance of IDA erythrocytes infected with malaria parasites. (A) Macrophages isolated from the indicated mice were cultured with CFSE-labeled parasitized erythrocytes (bottom panels) obtained from iron-sufficient mice infected with PyL. Two hours later, macrophages were analyzed for their capacity to ingest erythrocytes using flow cytometry. The numbers represent the mean percentages of $CD11b^+$ macrophage-engulfed erythrocytes from three individual experiments. (B) Peritoneal and (C) splenic macrophages isolated from iron-sufficient, uninfected mice were cultured with CFSE-labeled erythrocytes isolated from the indicated mice. Phagocytosis was assessed as above. All experiments were performed in triplicate. (D) Mice were transfused with CFSE-labeled schizont-infected erythrocytes (top panel) or with schizont-free erythrocytes (middle panel) isolated from control (filled columns) and IDA mice infected with PyL (open columns). Mice were given erythrocytes from uninfected recipients (bottom panel). Peripheral blood was collected and analyzed for $CFSE^+$ cells using flow cytometry at the indicated time points after inoculation. Values represent means ± SD ($n = 3$) of the percentage of the transfused erythrocytes within the whole erythrocyte population in the circulation. Asterisks indicate significant differences between IDA and control erythrocytes. (E) Splenic macrophages, isolated from mice injected with the indicated cells labeled with CFSE, were analyzed for phagocytosis in vivo 90 min after injection. Data represent the mean ($n = 3$) of the percentages within each quadrant. Two repeated experiments showed similar results.

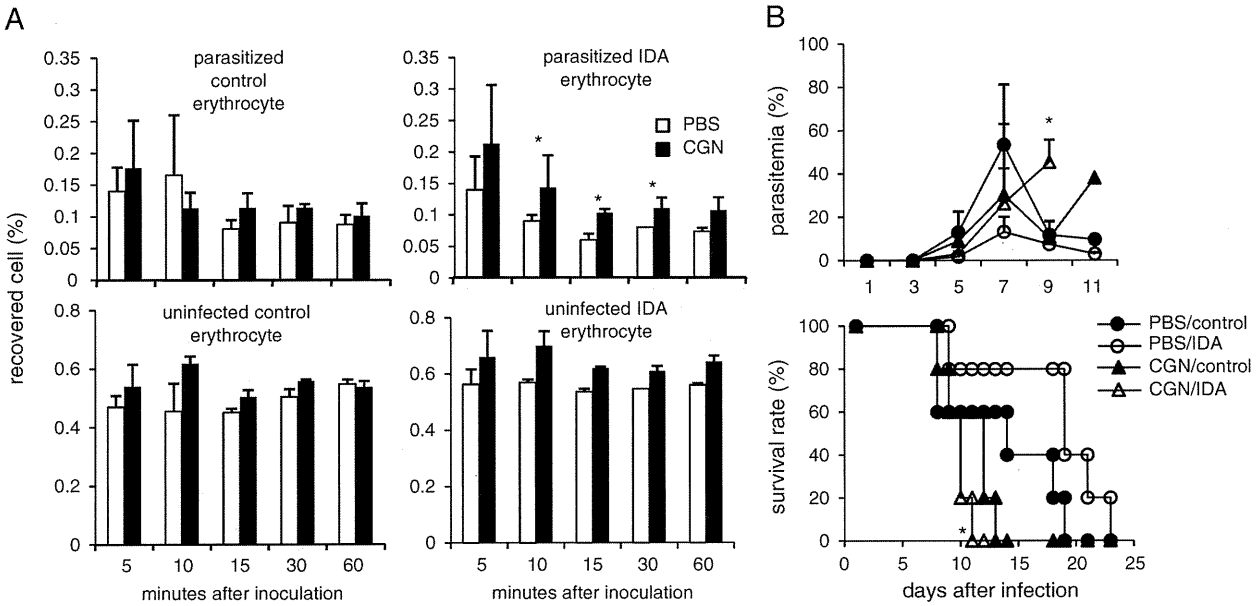

Figure 5. Reversal of resistance to Py by inhibiting macrophage phagocytosis. (A) Mice treated with (filled columns) or without CGN (open columns) were inoculated with uninfected (bottom) or infected erythrocytes (upper) isolated from iron-sufficient (left panels) or IDA mice (right panels). Transfused cells were analyzed as in Fig. 4D. (B) To evaluate the effects of blocking phagocytosis on the resistance to malaria, control (filled symbols) and IDA mice (open symbols) treated with (triangles) or without (circles) CGN were infected with PyL. Parasitemia and survival rate were monitored. Values for parasitemia are arithmetic means ± SD from six mice in each group. Asterisks indicate significant differences in parasitemia (upper panel) or in survival (lower panel) between IDA mice treated with or without CGN. Two repeated experiments showed similar results.

responsible for the changing the composition between the outer and inner leaflets of the plasma membrane lipid bilayer are scramblase, flippase and floppase (aminophospholipid translocase (APT)). Scramblase, located under the inner monolayer, carries inner phospholipids to the outer monolayer following an increase in cytosolic Ca^{2+} concentration. Some studies report that erythrocytes infected with malaria parasites show substantial increases in Ca^{2+} concentration [16], which led us to examine the Ca^{2+} concentration in IDA erythrocytes. As shown in Fig. 7, fluorescence microscopic analyses of erythrocytes stained with the Ca^{2+} indicator, Flou-4/AM, revealed a marked accumulation of Ca^{2+} in the cytosolic spaces within parasitized IDA erythrocytes, whereas those from iron-sufficient mice showed limited increases in Ca^{2+} associated with the nuclei (parasites).

Discussion

Iron deficiency, leading to a typical microcytic hypochromic anemia, is a widespread and common nutritional problem in developing countries. Many people suffer from IDA in areas that are endemic for malaria [2], and it is known that IDA individuals are protected against malaria. Because IDA influences sporozoite development in the liver [17], it is possible that the severity of the blood-stage infection might be modified in humans due to alterations during the earlier stages; however, in this study, we found that IDA mice were highly resistant to erythrocytic-stage

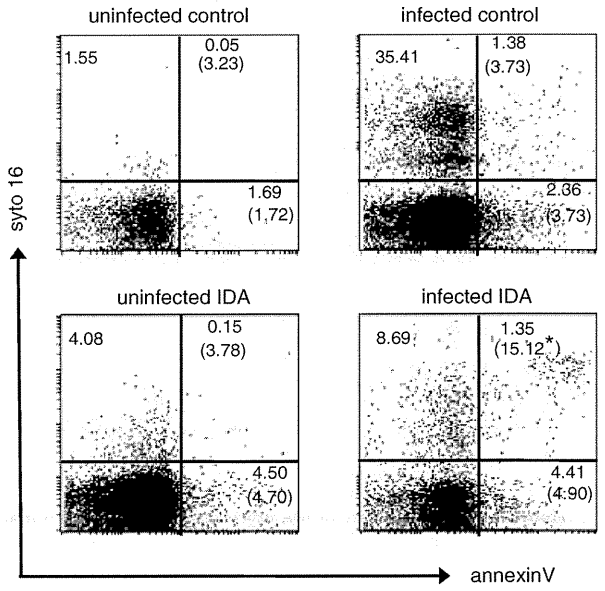

Figure 6. Increased phosphatidylserine exposure in IDA erythrocytes infected with Py. Gated $TER119^{+}CD71^{-}$ erythrocytes from IDA or control mice infected with PyL were stained 9 days after infection with annexin V and Syto 16. The numbers indicate the mean ratios within each quadrant. Numbers in parentheses indicate ratio of annexin V binding cells to parasitized (upper right) or uninfected erythrocytes (lower right) from three mice. The ratio of annexin V^{+} cell:parasitized cells in IDA mice (asterisk) was significantly higher than that in control mice. Three repeated experiments showed similar results.

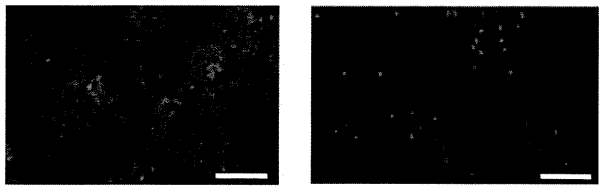

Figure 7. Evaluation of intracellular Ca^{2+} concentrations in erythrocytes from IDA mice. Erythrocytes from IDA or control mice infected with PyL were obtained and analyzed. Intracellular Ca^{2+} was visualized using Fuol-4/AM dye (green) under a fluorescence microscope. Parasite nuclei were stained with Hoechst stain (blue). Scale bars indicate 10 μm (original magnification: × 600). Three repeated experiments showed similar results.

malaria, and we addressed the mechanisms underlying resistance to malaria in IDA.

First, we analyzed whether IDA affects the intra-erythrocytic development of the parasites. PyL parasites grew and proliferated in IDA erythrocytes in a manner comparable with that in control erythrocytes, even when cultured in the presence of low levels of iron (Fig. 2A). The resulting schizont-infected IDA erythrocytes contained similar numbers of intracellular merozoites to those in control erythrocytes (Fig. 2B). An alternative possibility is that IDA erythrocytes are more resistant to parasite invasion. Although we could not test this because of technical limitations in the use of murine parasites [18], it is unlikely, as Luzzi et al. proved, that *P. falciparum* invades IDA erythrocytes to the same degree as control erythrocytes [19]. Thus, we speculated that IDA does not adversely affect the parasites themselves and that resistance in IDA might be associated with host protective mechanisms.

In addition to the lower levels of parasitemia during the very early phase of infection, acquired immunity is not well developed, suggesting that primitive protective mechanisms may operate. Indeed, we found that parasitized IDA cells were more susceptible to engulfment by phagocytes than control cells in vitro, resulting in rapid clearance from the circulation (Fig. 4). Furthermore, inhibition of phagocytosis slowed the clearance of parasitized IDA cells and abrogated resistance to infection by PyL in IDA mice (Fig. 5), demonstrating that the resistance observed in IDA mice was mainly dependent on phagocytosis. Our findings also showed that phagocytosis of ring-stage parasites, prior to the development of parasites capable of sequestration (Fig. 1C, Fig. 4D), may account for the reduced incidence of severe malaria in IDA patients. It would be interesting to investigate this using a model of experimental cerebral malaria.

We speculated that the higher susceptibility of IDA erythrocytes to phagocytosis results from the exposure of PS during parasite development, although we could not prove this experimentally. As apoptotic nucleated cells are phagocytosed after recognition by macrophages expressing receptors specific for PS [20], erythrocytes with exposed PS might be taken up by these macrophages. Several conditions, including aging, induce PS exposure in erythrocytes resulting in their rapid clearance [14]. Iron-deficiency may also increase PS exposure. One possible mechanism is that IDA erythrocytes have reduced levels of glutathione peroxidase, leading to higher sensitivity to oxidative stress, a major cause of PS externalization by erythrocytes [21]. Oxidative stress also induces alterations in band 3 in erythrocytes, resulting in them being recognized and phagocytosed by macrophages in a PS-independent manner [22].

Another possibility is that the enzymes involved in PS exposure are altered in IDA. Externalization of PS is regulated by three enzymes: a Ca^{2+}-dependent scramblase, which catalyzes the bidirectional movement of phospholipids across the lipid bilayer; an ATP-dependent APT, which mediates the energy-dependent transfer of phospholipids from the outer to the inner leaflet; and a third enzyme that mediates the energy-dependent transfer of phospholipids from the inner to the outer leaflet [23]. It is reported that activation of scramblase and dysfunction of APT are responsible for PS exposure in erythrocytes [24, 25]. We observed that cytosolic Ca^{2+}concentrations increased in parasitized IDA erythrocytes, which may indicate scramblase activation. Measuring ATP concentrations would be interesting to deduce the activity of APT. Increases in Ca^{2+}concentration also activate calpain, a protease that degrades spectrin [26], which might affect the structure and the susceptibility of erythrocytes to phagocytosis.

As previously reported [2, 4], we found that T-cell responses in IDA mice were decreased (Fig. 3A–C). In general, iron-deficiency results in impaired immunity, mainly because the enzymes regulating immune responses and DNA replication require iron [27]. In addition to the lack of iron, activation of Tregs may participate in downregulation of T-cell-mediated immunity. Tregs from IDA mice showed enhanced suppressive functions (Fig. 3D) presumably related to PS-mediated phagocytosis of parasitized IDA erythrocytes. Because PS receptors are responsible for the downregulation of inflammatory responses after uptake of apoptotic cells [20], activation of Tregs might be one of the immunosuppressive consequences of PS-mediated phagocytosis. Indeed, an immunosuppressive cytokine crucial for Treg function, TGF-β, is vigorously produced during phagocytosis of apoptotic cells [20]. Furthermore, Kleinclauss et al. reported that Tregs are involved in the protective effects seen after apoptotic cell administration in graft-versus-host disease [28]. Thus, it is quite possible that parasitized IDA erythrocytes with exposed PS have immunomodulatory characteristics.

In conclusion, parasitized IDA erythrocytes tend to be eliminated by phagocytic cells that sense alterations in the membrane structure of parasitized erythrocytes. Resistance to malaria in patients with hemoglobin variants is partially explained by the higher susceptibility of mutant erythrocytes to phagocytosis [29–31]. Here, we provide the first in vivo evidence that phagocytosis of parasitized erythrocytes is critical for resistance to malaria in IDA mice. Evaluation of whether this is the case in humans is important for the development efficient therapeutic strategies for both malaria and IDA.